# Hygroscopicity of particles generated from photooxidation of α-pinene under different oxidation conditions in the presence of sulfate seed aerosols

Biwu Chu[1,2], Kun Wang[1], Hideto Takekawa[3], Junhua Li[1], Wei Zhou[1],
Jingkun Jiang[1], Qingxin Ma[2], Hong He[2], Jiming Hao[1,*]

1. State Key Joint Laboratory of Environment Simulation and Pollution Control, School of Environment, Tsinghua University,
Beijing 100084, China. E-mail: bwchu@rcees.ac.cn
2. Research Center for Eco-Environmental Science, Chinese Academy of Sciences, Beijing 100085, China
3. Toyota Central Research and Development Laboratory, Nagakute, Aichi, 480-1192, Japan

## ARTICLE INFO

## ABSTRACT

Smog chamber experiments were conducted to investigate the hygroscopicity of particles generated from photooxidation of α-pinene/NO$_x$ with different sulfate seed aerosols or oxidation conditions. Hygroscopicity of particles was measured by a tandem differential mobility analyzer (TDMA) in terms of hygroscopic growth factor ($Gf$), with a relative humidity of 85%. With sulfate seed aerosols present, $Gf$ of the aerosols decreased very fast before notable secondary organic aerosols (SOA) formation was observed, indicating a heterogeneous process between inorganic seeds and organic products might take place as soon as oxidation begins, rather than only happening after gas-aerosol partition of organic products starts. The final SOA-coated sulfate particles had similar or lower $Gf$ than seed-free SOA. The hygroscopicity of the final particles was not dependent on the thickness but on the hygroscopicity properties of the SOA, which were influenced by the initial sulfate seed particles. In the two designed aging processes, $Gf$ of the particles increased more significantly with introduction of OH radical than with ozone. However, the hygroscopicity of SOA was very low even after a long time of aging, implying that either SOA aging in the chamber was very slow or the $Gf$ of SOA did not change significantly in aging. Using an aerosol composition speciation monitor (ACSM) and matrix factorization (PMF) method, two factors for the components of SOA were identified, but the correlation between SOA hygroscopicity and the proportion of the more highly oxidized factor could be either positive or negative depending on the speciation of seed aerosols present.

## Introduction

Hygroscopicity is one of the most important properties of atmospheric aerosols. First, atmospheric aerosols have both direct and indirect effects on climate change by interacting directly with radiation and changing cloud properties (IPCC, 2013). The magnitude of both direct and indirect effects depends strongly on aerosol hygroscopicity, which is usually described as the amount of water absorbed by a particle with a given dry diameter at a given relative humidity (RH). Water uptake affects particle size and therefore influences its optical properties (Cappa et al., 2011; Flores et al., 2012). In addition, the ability of a particle to serve as a cloud condensation nucleus (CCN) is highly dependent on its hygroscopic behavior (Michaud et al., 2009). Secondly, particle size and phase change due to water uptake also influence many physicochemical characteristics of the aerosol, including respiratory tract deposition (Broday and Georgopoulos, 2001), atmospheric lifetime, and chemical reactivity (Heintzenberg et al.,

* Corresponding author. E-mail: hjm-den@tsinghua.edu.cn

2001), especially with respect to heterogeneous chemistry.

Aerosol hygroscopicity is usually measured with a tandem differential mobility analyzer (TDMA). According to the diameter growth of aerosols, a growth factor ($Gf$) can be calculated to characterize the hygroscopicity of aerosols:

$$Gf = d_p/d_{p0} \qquad (1)$$

where, $d_{p0}$ is the diameter of the initial dry aerosols, and $d_p$ is the diameter of the humidified aerosols after absorbing water in a TDMA with controlled RH, respectively. Atmospheric aerosols are always mixtures. The hygroscopicity of aerosols depends on their composition as well as the mixing state of the aerosol. The $Gf$ of the mixture of particles can be calculated from the volume fraction of each component, i.e. the Zdanovskii-Stokes-Robinson (ZSR) model (Stokes and Robinson, 1966):

$$Gf_{mixed} = (\sum (X_i \times Gf_i^3))^{1/3} \qquad (2)$$

where, $Gf_{mixed}$ is the $Gf$ of the mixed particles, and $X_i$ and $Gf_i$ are the volume fraction and $Gf$ of component $i$ respectively.

Generally, the ZSR model can be applied only to well-mixed particles and has limitations for core-shell particles. For example, Xiong et al. (1998) suggested that a surface organic layer would suppress the ability of an internal inorganic material to absorb water. Mochida et al. (2008) found that aerosol hygroscopicity in the Tokyo area would be significantly decreased with photochemical processing, indicating that newly generated organic components coated the hydrophilic pre-existing aerosols, and reduced their hygroscopicity. However, Virkkula et al. (1999) thought that the $Gf$ of particles was inversely proportional to the organic volume fraction when seed aerosols were present, but had no obvious relationship with the thickness of the organic layers.

The hygroscopicity of organic aerosols and mixed inorganic and organic aerosols remains uncertain. Generally, organic materials, especially newly generated organic aerosols or artificial organic aerosols in laboratory, are almost hydrophobic compared to inorganic aerosols. For example, Varutbangkul et al. (2006) measured that the $Gf$ at 85% RH of secondary organic aerosols (SOA) generated from photooxidation of sesquiterpene to be lower than 1.05. Virkkula et al. (1999) measured the hygroscopicity of SOA generated from ozonolysis of α-pinene and found their $Gf$ at 84% RH to be around 1.07. However, organic aerosol compositions are not always hydrophobic, but can influence and contribute significantly to the hygroscopicity of atmospheric aerosols according to field observation. Dick et al. (2000) found that the measured $Gf$ of atmospheric particles were significantly higher than the values predicted by the ZSR model, and the discrepancy increased with increasing fraction of organics. Gysel et al. (2004) investigated the hygroscopicity of atmospheric aerosols in a rural area. The ZSR model prediction could not agree with observation until they introduced some highly hydrophilic organic compositions instead of using $Gf$ of only 1.08–1.17 at 90% RH for organics. These observations indicated that some highly hydrophilic organic components exist in the atmosphere. Their high hygroscopicity might be the result of continuous aging processes in the atmosphere.

Increase of the hygroscopicity of organic aerosols in oxidation processes has been reported in a laboratory study. Cocker et al. (2001) found that the hygroscopicity of SOA generated from photooxidation of m-xylene or 1,3,5-trimethylbenzene or from the ozonolysis of α-pinene were increased by the oxidation process at the beginning of the reaction. The hygroscopicity change of SOA in the aging process may be explained by either additional SOA generation or change of the chemical composition (Tritscher et al., 2011). SOA property changes may occur either by heterogeneous reactions on particle surfaces or by condensed-phase reactions, such as functionalization, oligomerization, fragmentation and so on (Tritscher et al., 2011). However, in a previous study, laboratory aging only led to a limited increase in the hygroscopicity of SOA (Baltensperger et al., 2005). Thus, the aging of SOA in different oxidation conditions might need to be investigated.

Besides absorbing water by themselves, organic components also influence the hygroscopicity of inorganic aerosols. For example, Quinn et al. (2005) found that the optical properties of aerosols with a high fraction of organics depend less on RH. Sometimes, organic components can also increase the hygroscopicity of inorganic aerosols. It is well known that some inorganic salts will not absorb water until RH is higher than a threshold. The critical value of this threshold RH is defined as the deliquesce relative humidity (DRH). The DRH of $(NH_4)_2SO_4$ is 79.5%. Meyer et al. (2009) found that organic components decreased the DRH of $(NH_4)_2SO_4$. Thus, in the presence of organics, $(NH_4)_2SO_4$ aerosols would deliquesce and show obvious hygroscopic growth below the normal DRH. Meanwhile, inorganic aerosols also affect organic aerosol formation in atmospheric chemical processes. In the past decades, many researchers observed that SOA formation was enhanced in the presence of acid seed aerosols (i.e. $(NH_4)_2SO_4$ and $H_2SO_4$) (Jang et al., 2002; Kroll et al., 2007; Lu et al., 2009). Recently, some metallic salts were also found to have significant effects on SOA formation (Chu et al., 2012, 2013). The interaction between inorganic aerosols and organic compounds and its effects on hygroscopic properties of particles are not yet fully understood.

Therefore, we measured SOA hygroscopicity and their chemical composition in photooxidation experiments with different sulfate seed aerosols or oxidation conditions. Analysis of the relationship between experimental con-

ditions and hygroscopicity of the generated particles, as well as time variation of the chemical composition and hygroscopic $Gf$ of SOA in the experiments, is provided in this article.

# 1 Methods

Photooxidation experiments were carried out in a smog chamber described in detail in Wu et al. (2007). The reactor is a 2-m$^3$ cuboid reactor, constructed with 50 μm-thick FEP-Teflon film (Toray Industries, Inc. Japan) and irradiated by 40 black lights (GE F40T12/BLB, peak intensity at 365 nm). Based on the equilibrium concentrations of NO, NO$_2$, and O$_3$ in a photo-irradiation experiment of an NO$_2$/air mixture, the NO$_2$ photolysis rate was calculated at approximately 0.21 min$^{-1}$, using a method described by Takekawa et al. (2000, 2003). Since temperature (Takekawa et al., 2003) and RH (Prisle et al., 2010) could have significant influence on SOA formation, all experiments were carried out at a temperature of 30 ± 0.5°C and 48.5%–50.5% RH in this study.

Before experiments started, inorganic seed aerosols were generated by atomizing 1 mg/L salt solutions using a constant output atomizer (TSI Model 3076). The generated aerosols were passed through a diffusion dryer (TSI Model 3062) to remove water and a neutralizer (TSI Model 3077) to bring the aerosols to an equilibrium charge distribution.

In this study, (NH$_4$)$_2$SO$_4$, FeSO$_4$ and ZnSO$_4$ were chosen as representatives of sulfate. The size range of these polydisperse seed aerosols was about 30–300 nm, with count median diameters (CMD) about 85–90 nm. In addition, α-pinene was injected into a vaporizer and then carried into the chamber by purified air, while NO$x$ were injected into the chamber from standard gas bottles directly.

In each experiment, particle generation was calculated from the particle size distribution, which is measured by a scan mobility particle sizer (SMPS, TSI Model 3936). Wall deposition of particles was corrected followed the method developed by Takekawa et al. (2003) as described in detail in our previous study (Chu et al., 2012). Since we did not measure the density of the generated SOA, we used volume concentration to express SOA generation. The hygroscopicity and chemical composition of aerosols was measured by a home-built TDMA and an aerosol composition speciation monitor (ACSM). The TDMA was built from the SMPS and an additional differential mobility analyzer (DMA, TSI Model 3081). A schematic of the TDMA is shown in **Fig. 1**. DMA I was used to select 150 nm dry aerosols. DMA II and CPC were used to measure the size distribution of the aerosols after their hygroscopic growth in the Nafion tube. The TDMA was characterized and tested, including measuring the diameters of polystyrene latex (PSL) aerosols and the hygroscopic growth curve of (NH$_4$)$_2$SO$_4$ (**Figs. S1 and S2**). The hygroscopic growth curve agreed well with previous studies (Cruz and Pandis, 2000; Ma et al., 2010),



**Fig. 1** Schematic of TDMA system.

indicating that the TDMA could measure *Gf* of aerosols accurately. ACSM is a simplified version of aerosol mass spectrometry (AMS), with similar principles and structure. Ng et al. (2011) presented a detailed introduction to this instrument and found the measurement results agreed well with AMS.

# 2 Results and discussion

## 2.1 Hygroscopicity of SOA in photooxidation of α-pinene/NO*x* in the absence or presence of sulfate seeds

The hygroscopicity of seed-free SOA generated from α-pinene photooxidation was reported previously (Duplissy et al., 2008; Juranyi et al., 2009; Varutbangkul et al., 2006; Virkkula et al., 1999) and was also measured in this study. Experimental conditions and measured results are summarized in **Table 1**. In order to compare hygroscopic *Gf* with different RH, Petters and Kreidenweis (2007) developed a single parameter, $\kappa$, to represent hygroscopic growth properties, which was also calculated and shown in **Table 1**. The parameter $\kappa$ is defined through the effect of particulate matter on the water activity of the solution. Lower values of $\kappa$ indicate less hygroscopic, or less CCN-active, behavior of particles. Seed-free SOA generated from α-pinene photooxidation had only very limited hygroscopic growth when RH was lower than 85%. Notable growth

did not occur unless water vapor was near saturation. The *Gf* of pure SOA in this study were about 1.03–1.09 with 85% RH, and the hygroscopic growth parameters $\kappa$ were calculated to be 0.018–0.056. These values were similar to those found in Varakutbangkul's experiments, which were carried out under experiment conditions similar to this study. In addition, we also found the *Gf* of SOA generated from high concentration α-pinene was lower than that from low concentration α-pinene. This could be explained by the partitioning of less hygroscopic organic compounds. A high concentration of α-pinene resulted in a high concentration of organic aerosol. Thus some organic gas with relatively high volatility would partition into the aerosol phase, according to partition theory (Odum et al., 1996). These organic compounds were always less oxidized and less hygroscopic than the compounds that could partition to the aerosol phase at a low concentration of organic aerosol. Therefore, the hygroscopicity of SOA would decrease with increasing concentration of α-pinene.

Besides seed-free SOA, the hygroscopicity of SOA-coated sulfate particles was also investigated. Experiments of α-pinene/NO*x* photooxidation were conducted in the presence of $(NH_4)_2SO_4$, $FeSO_4$, or $ZnSO_4$. The experimental conditions and the *Gf* of the SOA-coated particles after 4 hours' reaction in these experiments are listed in **Table 2**. In these experiments with presence of sulfate seed aerosols, no significant new particle formation was observed according to SMPS measurement, indicating that SOA mainly condensed on the surface of the sulfate seed aerosols.

| **Table 1** Hygroscopicity of pure SOA generated from α-pinene photooxidation | | | | | | | | |
|---|---|---|---|---|---|---|---|---|
| $C^0_{\alpha\text{-pinene}}$ (ppmV) | Temp. (K) | RH (%) | NO*x* (ppbV) | $d_{p0}$ (nm) | *Gf* | Measured RH (%) | $\kappa$ | Reference |
| 0.10 | ~293 | < 1 | 18–300 | 50–120 | 1.09 | 84 | 0.062–0.070* | Virkkula et al., 1999 |
| 0.12 | ~293 | 50 | 120 | 180 | 1.09 | 85 | 0.056* | Varutbangkul et al., 2006 |
| 0.010–0.18 | NA | NA | NA | NA | 1.13–1.42 | 95 | NA | Duplissy et al., 2008 |
| 0.01–0.03 | 293 | 50–60 | 5–13.5 | 200 | 1.63 | 97 | 0.126 | Juranyi et al., 2009 |
| 0.22–0.27 | 293 | 50–60 | 110–135 | 200 | 1.43 | 97 | 0.074 | |
| 0.04 | 303 | 50 | 100 | 150 | 1.09 ± 0.010 | 85 | 0.056 | This study |
| 0.20 | 303 | 50 | 100 | 150 | 1.03 ± 0.011 | 85 | 0.018 | |

* Calculated followed the method developed by Petters and Kreidenweis (2007). RH: relative humidity.

| **Table 2** Experimental conditions and *Gf* values | | | | | | |
|---|---|---|---|---|---|---|
| Experiment No. | $C^0_{\alpha\text{-pinene}}$ (ppmV) | Seeds | $PM_0$ (μm³/cm³) | CMD (nm) | $NO_0$ (ppbV) | $NO_{2,0}$ (ppbV) | *Gf* (RH = 85%) |
| 0.04-10A | 0.04 | $(NH_4)_2SO_4$ | 10.1 | 88.5 | 51 | 48 | 1.13 |
| 0.08-10A | 0.08 | $(NH_4)_2SO_4$ | 11.7 | 87.9 | 49 | 53 | 1.05 |
| 0.2-10A | 0.20 | $(NH_4)_2SO_4$ | 12.3 | 87.1 | 52 | 55 | 1.05 |
| 0.2-10F | 0.20 | $FeSO_4$ | 9.3 | 85.0 | 48 | 56 | 1.00 |
| 0.2-10Z | 0.20 | $ZnSO_4$ | 10.2 | 89.4 | 52 | 55 | 1.02 |

Experimental No. was designed to follow the format of α-pinene concentration-concentration and name of initial letter of the seed aerosol. 0.04-10 A represents an experiment with initial 0.04 ppmV α-pinene and 10 μm³/cm³ $(NH_4)_2SO_4$ seed aerosol.

Time variation of the hygroscopic $Gf$ with 85% RH for the generated particles in the first three experiments in **Table 2** is shown is **Fig. 2**. Before reaction started, the $Gf$ of $(NH_4)_2SO_4$ seeds was about 1.54, and it quickly decreased when the reaction started. The immediately falling of the $Gf$ indicated that either SOA was generated as soon as the irradiation began, or $(NH_4)_2SO_4$ seed aerosol was involved in the primary oxidation process of α-pinene. Since SOA formation would not occur before gas phase products accumulated, and we did not see obvious SOA formation until after irradiating the reactor for 0.5 hr, as shown in **Fig. 2**, the latter hypothesis was more reasonable. Therefore, some reaction or uptake occurred on the surface of the $(NH_4)_2SO_4$ aerosol and decreased its hygroscopicity. In **Fig. 3**, we also observed a similar phenomenon on $ZnSO_4$ and $FeSO_4$ aerosols. This phenomenon also indicated the importance of heterogeneous processes on the surface of the inorganic seed aerosol in SOA formation. Heterogeneous processes between inorganic seeds and organic products might take place as soon as oxidation begins, rather than only happening after gas-solid partition.

As shown in **Fig. 2**, the initial experimental conditions of the three experiments were similar except for the initial concentrations of α-pinene. A different concentration of α-pinene resulted in a different concentration of SOA, and therefore, a different thickness of the organic coating layer on the surface of $(NH_4)_2SO_4$ seeds. The $Gf$ of particles in the experiment with 0.20 ppmv α-pinene decreased to a minimum value in 0.5 hours and then remained stable. The final $Gf$ of the particles was similar to that of seed-free SOA. Similar results were obtained in the experiment with 0.08 ppmv α-pinene, but the $Gf$ of the particles decreased more slowly to a minimum final $Gf$ than in the experiment with 0.20 ppmv α-pinene. The more slowly decreasing rate of the $Gf$ might due to the lower concentration of gas phase organic products with lower concentration of α-pinene. In experiment "0.04-10A", the initial concentration
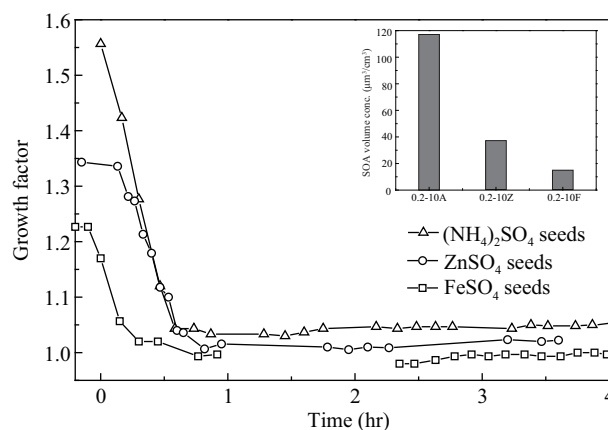
**Fig. 3** Time variation of hygroscopicity of SOA-coated $(NH_4)_2SO_4$, $FeSO_4$ or $ZnSO_4$ seed aerosols (full picture, $d_{p0}$ = 150 nm), and SOA yields in experiments in the presence of $(NH_4)_2SO_4$, $FeSO_4$ or $ZnSO_4$ seed aerosols (inner picture).

of α-pinene was 0.04 ppmv, and the final value of the $Gf$ in this experiment was higher than that in the other two experiments. The higher final value of the $Gf$ in the experiment with the lowest concentration of α-pinene might be attributed both to a thinner SOA coating and the higher hygroscopicity of the SOA.

In the last three experiments in **Table 2**, the initial conditions were similar except for the seed species. We introduced a high concentration of α-pinene to provide a high enough SOA coating thickness, in order to conceal the hygroscopic growth of the sulfate seeds themselves. Time variations of hygroscopicity of SOA-coated particles in these three experiments are shown in **Fig. 3**. Before irradiation started, the $Gf$ of $FeSO_4$ and $ZnSO_4$ seeds were about 1.23 and 1.34 respectively. As soon as photooxidation started, the $Gf$ of particles decreased quickly to a minimum value in less than an hour and then remained stable in the three experiments. The final particles had very low hygroscopicity in all three experiments. Their hygroscopic $Gf$ with 85% RH were less than 1.05, and the corresponding hygroscopic growth parameters $\kappa$ were less than 0.031. These values were similar or even lower than that of the SOA generated in seed-free experiments under similar experimental conditions.

The final $Gf$ of particles in experiments with three kinds of sulfate seed aerosols followed exactly the order of the hygroscopicity of the initial seed aerosols. The reason for this phenomenon could be either differences in the thickness or hygroscopicity of the SOA coating. We measured the SOA volume concentrations in these three experiments, which are shown in the inner picture in **Fig. 3**. Due to the enhancing effects of $(NH_4)_2SO_4$ seed aerosols (Lu et al., 2009) and the suppressing effects of $FeSO_4$ seed aerosols (Chu et al., 2012) on SOA formation, experiments with $(NH_4)_2SO_4$ seed aerosols had the highest SOA concentration, while the lowest concentration of SOA was generated in experiments with $FeSO_4$ seed aerosols. A higher SOA

**Fig. 2** Time variation of growth factor of SOA-coated $(NH_4)_2SO_4$ seeds ($d_{p0}$ =150 nm) with sulfate seed aerosols present and SOA formation in experiment 0.2-10A. SOA concentrations in experiments 0.04-10A and 0.08-10A were low and had high uncertainty due to wall deposition.

concentration would cause a thicker SOA coating layer on the surface of sulfate seed aerosols, since the initial surface concentrations of $(NH_4)_2SO_4$, $FeSO_4$ or $ZnSO_4$ seed aerosols were similar. All three sulfate seed aerosols had higher hygroscopicity than the SOA, so SOA coating would decrease the $Gf$ of the seed particles. The $Gf$ of the SOA-coated sulfate particles would be lower when the SOA concentration was high if the hygroscopicity of the particles was controlled by SOA thickness. However, the observed results followed the reverse order. Thus we believe that in all the experiments, the SOA layers were thick enough that the core sulfate seed had little contribution to the hygroscopicity of the particles. The hygroscopicity of SOA-coated sulfate particles was not dependent on the thickness of the SOA, but on its hygroscopicity properties. In our previous study, we speculated that some oxidized compositions could be reduced by $FeSO_4$ seed aerosols (Chu et al., 2012). Since oxidized compositions always had higher hygroscopicity than reduced products, $FeSO_4$ seed aerosols should decrease the hygroscopicity of the SOA. This explained the observation that SOA with $FeSO_4$ seed aerosols had the lowest hygroscopicity.

## 2.2 SOA generation with further oxidation

In real atmospheric environments, particles always undergo complicated aging processes, during which the physical and chemical properties of particles may change a great deal. In this study, both seed-free SOA and SOA-coated sulfate particles had very low hygroscopicity, which might be due to a lack of aging. So we investigated the change of hygroscopicity of the particles in subsequent oxidation processes to simulate hygroscopicity changes in aging. In this study, two aging processes were designed and designated as "365" and "254", respectively. In process "365", the experimental conditions remained the same as for photooxidation, so the main oxidant in this aging process was accumulated $O_3$ in the first 4 hours of photooxidation. In process "254", we generated OH radical in the system by injecting $H_2O_2$ and irradiating the system with 254 nm black light:

$$H_2O_2 + hv \ (254 \ nm) \longrightarrow 2OH\cdot \tag{3}$$

The experimental conditions of photooxidation and further oxidation process are listed in **Table 3**.

The time variation of generated SOA in photooxidation and process "254" are shown in **Fig. 4**. In the first four hours in **Fig. 4**, all experiments were irradiated by 365 nm light except experiment "Seed-free-254". After 4 hours of reaction under 365 nm light, all initial α-pinene was consumed and the particle concentration became stable. The differences of the curves in this period indicated an
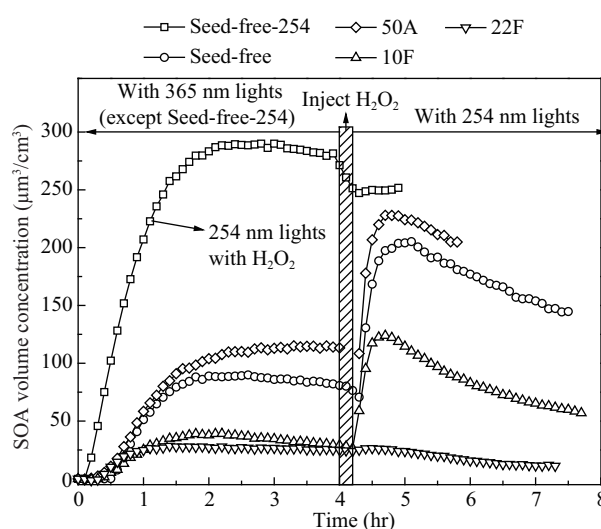
**Fig. 4**    SOA generation in photooxidation of α-pinene and further oxidation with 254 nm light.

**Table 3**    Experimental conditions for photooxidation of α-pinene with further oxidation process

| Experiment No. | HC$_0$ (ppmV) | Sulfate seed concentration (μm$^3$/cm$^3$) | NO$_0$ (ppbV) | NO$_{2,0}$ (ppbV) | Light(before 4 hr)(nm) | H$_2$O$_2$ injection* (ppmV) | Light(after 4 hr) (nm) |
|---|---|---|---|---|---|---|---|
| Seed-free-254 | 0.20 | None | 44 | 49 | 254 | ~1 | 254 |
| Seed-free-365 | 0.20 | None | 49 | 49 | 365 | 0 | 365 |
| Seed-free | 0.20 | None | 51 | 47 | 365 | ~1 | 254 |
| 10A-365 | 0.20 | $(NH_4)_2SO_4$ (12.3) | 52 | 55 | 365 | 0 | 365 |
| 10A | 0.20 | $(NH_4)_2SO_4$ (12.9) | 55 | 45 | 365 | ~1 | 254 |
| 50A | 0.20 | $(NH_4)_2SO_4$ (49.6) | 49 | 57 | 365 | ~1 | 254 |
| 10F-365 | 0.20 | $FeSO_4$ (9.3) | 48 | 56 | 365 | 0 | 365 |
| 10F | 0.20 | $FeSO_4$ (10.3) | 49 | 51 | 365 | ~1 | 254 |
| 22F | 0.20 | $FeSO_4$ (22.3) | 49 | 50 | 365 | ~1 | 254 |
| 10Z | 0.20 | $ZnSO_4$ (10.2) | 52 | 55 | 365 | ~1 | 254 |

* The injected $H_2O_2$ concentration was calculated by the injected amount of $H_2O_2$ and the volume of the reactor.

"Experiment No." was designed to follow the format [concentration and name initial letter of the seed aerosol]-[wavelength of lights, omitted if both 365 nm light and 254 nm light were used]. For example, "seed-free-254" represents a seed-free experiment under radiation of 254 nm light, and "10A" represents an experiment with 10 μm$^3$/cm$^3$ $(NH_4)_2SO_4$ seed aerosol present under radiation of 365 nm light in photooxidation and 254 nm light in aging.

enhancing effect of $(NH_4)_2SO_4$ and a suppressing effect of $FeSO_4$ seed aerosols on SOA formation compared to the seed-free experiment.

Significant additional SOA were generated after injecting $H_2O_2$ and turning on 254 nm light to generate OH radicals, while no notable particle formation was observed in process "365". In an experiment with only purified air under irradiation by 254 nm light and $H_2O_2$, about 40 $\mu m^3/cm^3$ particles were generated. The amount of additional particle formation in process "254" was similar in the seed-free experiment and the experiment with $(NH_4)_2SO_4$ seed aerosols, about 129 and 121 $\mu m^3/cm^3$ respectively. So the additional SOA formation was contributed by oxidation of both intermediate products of *a*-pinene and the purified air. However, additional SOA formation in experiments with $FeSO_4$ seed aerosols was about 92 $\mu m^3/cm^3$, which was lower than that in the seed-free experiment and the experiment with $(NH_4)_2SO_4$ seed aerosols. What is more, in the experiment with a high concentration of $FeSO_4$ seed aerosols, only about 5 $\mu m^3/cm^3$ additional SOA were generated. Thus $FeSO_4$ seed aerosols also showed a suppressing effect on aerosol formation in photooxidation with 254 nm light and $H_2O_2$.

After rapid additional SOA formation, some SOA components seemed to be depleted with the irradiation by 254 nm light. As shown in **Fig. 4**, the decrease could continue for 4 hr at least, but the remaining SOA was still higher than that before injecting $H_2O_2$ and turning on the 254 nm light. The reason for the decrease might be either oxidation or photolysis of some components in SOA under the irradiation by 254 nm light. After injecting $H_2O_2$ and turning on the 254 nm light, some components of the SOA might be oxidized or decomposed to smaller molecules, and then partitioned to the gas phase. We also

carried out an experiment (Seed-free-254) with irradiation by 254 nm light from the beginning of the reaction in the presence of $H_2O_2$. As shown in **Fig. 4** his experiment had the highest SOA formation, and the concentration did not change when we injected more $H_2O_2$ to generate more OH radicals in the reactor.

### 2.3 Hygroscopicity of SOA and SOA-coated particles during further oxidation process

We compared the hygroscopic *Gf* of particles generated from photooxidation of α-pinene and the additional oxidation process. The hygroscopic *Gf* of seed-free SOA are shown on the left side in **Fig. 5**. In aging process "365", no obvious change of hygroscopicity was observed. In process "254", as we discussed in the last paragraph, significant additional SOA formation occurred. Severe nucleation also took place in the aging process according to the size distribution of the particles. An example of the size distribution of particles is shown in **Fig. S3**. The particles we selected to measure hygroscopicity in process "254" were mainly newly-generated particles. The *Gf* of the newly generated particles was about 1.05, which was higher than that of the particles generated in the photooxidation with 365 nm light. In the subsequent aging in process "254", the *Gf* of the newly generated particles increased to about 1.12. A similar phenomenon was observed in experiments with sulfate seed aerosols present. The hygroscopic *Gf* of SOA-coated $(NH_4)_2SO_4$ and $FeSO_4$ particles are shown on the right side of **Fig. 5**. The hygroscopic *Gf* increased more significantly in process "254" than that in process "365". In some experiments, we investigated the hygroscopicity of SOA-coated sulfate seed aerosol for a long time (> 16 hr) of aging with 254 nm black light. The *Gf* of particles increased very slowly, as shown in **Fig. 6**, reflecting that
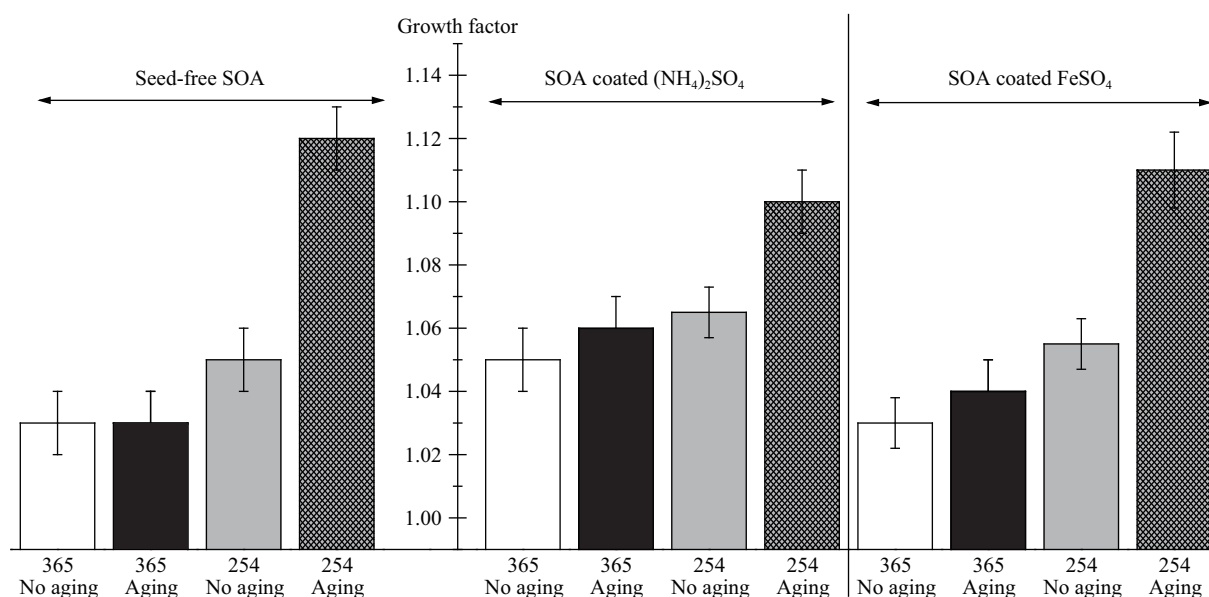


**Fig. 5**   Hygroscopicity of seed-free SOA and SOA-coated sulfate aerosols before and after aging.
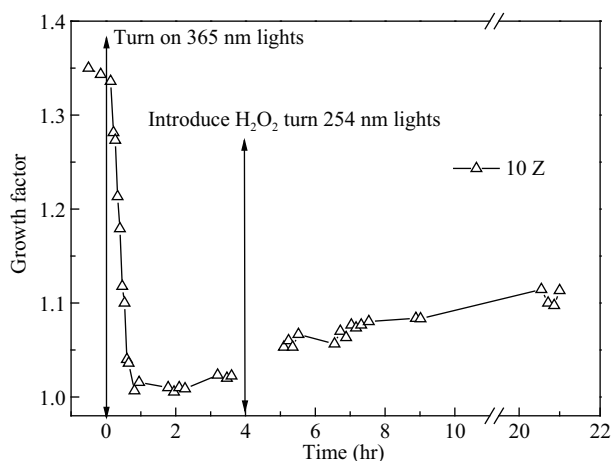
**Fig. 6** Time variation of growth factor of the SOA-coated ZnSO$_4$ seed aerosols ($d_{p0}$ = 150 nm) in photooxidation and subsequent aging process.

either SOA aging in the chamber was very slow or that the *Gf* of SOA did not change significantly during aging.

## 2.4 SOA composition and hygroscopicity

We believed that the observed hygroscopicity change of the particles was due to the change of their composition, and tried to identify the correlation between SOA hygroscopicity and composition. In this study, we used an ACSM to measure fragments with a mass to charge ratio (*m/z*) between 10 and 150. The measurement results of ACSM were analyzed using the positive matrix factorization (PMF) method. With the software developed by Ulbrich et al. (2009), two factors of the organic compounds in aerosol phase were indentified, marked as OA$_1$ and OA$_2$ respectively. Mass spectrometry data for these two factors are shown in **Fig. 7**. There were two main differences between these two factors: (1) the signal of *m/z* = 43 in OA$_1$ was higher than that in OA$_2$, while the signal of *m/z* = 28 and *m/z* = 44 was significantly lower than that in OA$_2$; (2) fragments of high *m/z* (> 60) in OA$_1$ was significantly higher than in OA$_2$.

We know that the signal of *m/z* = 43 is mainly contributed by fragments of hydrocarbon chains, i.e. C$_3$H$_7$, while the signals of *m/z* = 28 and *m/z* = 44 are mainly contributed
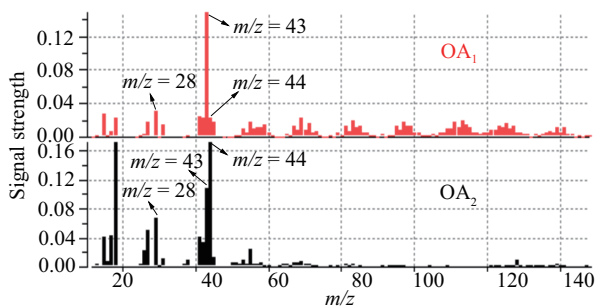
by fragments of aldehydes, ketones and carboxylic acids, i.e. CO and COO. Therefore, OA$_1$ could be considered to consist of less-oxidized organic products, and it was also contributed by some large molecules since it contained more fragments with high *m/z* value, while OA$_2$ could be considered to consist of more-oxidized organic products in the SOA. **Figure 7** shows time variations of OA$_1$ and OA$_2$ in the four experiments with the "254" aging process, including a seed-free experiment and three experiments with different sulfate seed aerosols. We did not carry out a deposition correction for the ACSM-measured results since we were concerned more about the proportion of OA$_1$ and OA$_2$ than their mass concentrations. The percentage of OA$_2$ in organic products (OA$_2$%) was used to reflect the oxidation degree of the SOA.

Time variations of OA$_1$, OA$_2$ and OA$_2$% are shown in **Fig. 8**. Most generated SOA at the beginning of photooxidation were OA$_1$. OA$_2$% was only about 15% at the end of photooxidation (4 hr). However, when the aging process started, OA$_2$% increased a great deal. As the aging process proceeded, concentrations of OA$_1$ and OA$_2$ in the reactor decreased due to both the deposition of particles on the reactor wall and depletion of SOA products as described earlier. An interesting phenomenon was that OA$_2$% also decreased after about 2 hours' aging. This indicated a higher depletion rate for OA$_2$ than OA$_1$. This was reasonable if SOA depletion was due to oxidation. OA$_2$, with a higher oxidation degree, should be more easily oxidized to small molecules. Additionally, oligomerization might also contribute to the decreasing of OA$_2$%. According to **Fig. 6**, larger molecules in SOA were classified into OA$_1$. Therefore, generation of oligomers would increase the OA$_1$ concentration. Since reactants of oligomerization were usually aldehydes and carboxylic acids (Gao et al., 2004; Hamilton et al., 2005), which were likely to be components in OA$_2$, OA$_2$% would decrease if oligomerization dominated aging.

The correlation between *Gf* of particles and OA$_2$% was analyzed. Since OA$_2$ had a higher oxidation degree and had more polar groups than OA$_1$, OA$_2$ should also be more hydrophilic than OA$_1$, and SOA hygroscopicity should increase with OA$_2$ fraction according to the ZSR model. The regression result showed that the two identified factors did not have clear or consistent differences in hygroscopicity; detailed discussion can be found in supplementary information. The more oxidized components in SOA, i.e. OA$_2$, were still not very hydrophilic in this study. One thing we must point out is that the measured SOA composition was the overall composition of SOA, while hygroscopicity or *Gf* was measured only for selected particles with a certain diameter. Measuring the corresponding composition of the selected particles with a certain diameter might be helpful to find the relationship between the composition and hygroscopicity of SOA in further study.
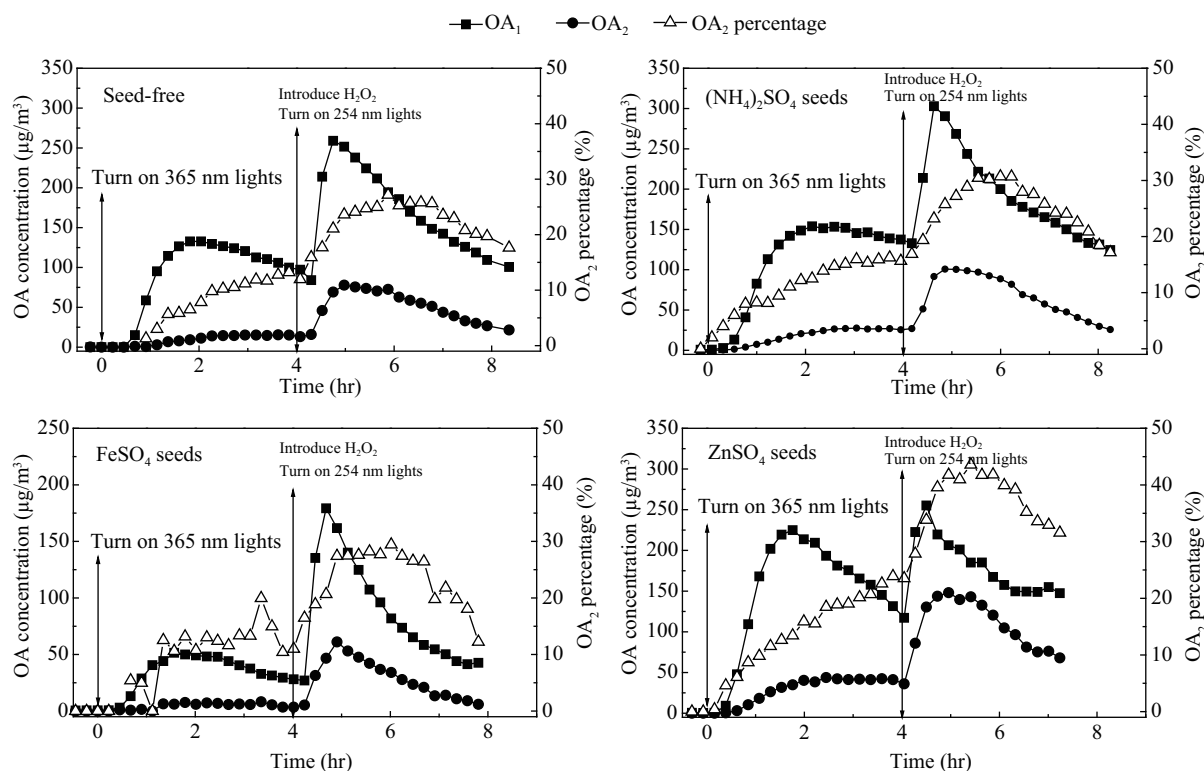


**Fig. 7** Mass spectrometry data for the two identified factors (OA$_1$ and OA$_2$) of the organic compounds in the aerosol phase.

**Fig. 8** Time variation of OA$_1$ and OA$_2$ and percentage of OA$_2$ during photo oxidation and aging in a seed-free experiment and in experiments with (NH$_4$)$_2$SO$_4$, FeSO$_4$ and ZnSO$_4$ seeds.

## 3 Conclusions

SOA generated from photooxidation of α-pinene/NO$x$ were hydrophobic. Their *Gf* with 85% RH was only 1.03–1.09. If sulfate seed aerosols were present, their hygroscopicity decreased very rapidly as soon as the photooxidation started and before significant SOA formation was observed. This indicated that (NH$_4$)$_2$SO$_4$ seed aerosol was involved in the primary oxidation process of α-pinene. And when α-pinene concentration was high enough (higher than 80 ppbV with 10 μm$^3$/cm$^3$ sulfate seed aerosols), the final particles (sulfate seed aerosols coated with SOA) had a hygroscopicity similar to seed-free SOA. The hygroscopicity of the final particles was not dependent on the thickness but on the hygroscopicity properties of the SOA. The hygroscopicity properties of SOA were influenced by the initial sulfate seed particles, so different sulfate seed particles resulted in different hygroscopicity properties for the final particles. Two aging processes were designed to investigate the hygroscopicity changes of SOA in the aging process. The hygroscopic *Gf* increased more significantly with introduction of OH radical than with ozone. However, the hygroscopicity of SOA in our experiments was very low even after a long time of aging, implying that either SOA aging in the chamber was very slow or the *Gf* of SOA did not change significantly with aging. We also measured the chemical composition of SOA during the photooxidation and the subsequent aging process with an aerosol composition speciation monitor (ACSM). Using the matrix factorization (PMF) method, two factors for the components of SOA were identified in photooxidation of α-pinene and the subsequent aging process. There was a trend that the proportion of the higher oxidized factor in SOA increased with the reaction and aging processes. However, the correlation between SOA hygroscopicity and the proportion of the more highly oxidized factor could be either positive or negative depending on the speciation of sulfate seed aerosols present. And according to our calculation, the more highly oxidized factor in SOA was still not very hydrophilic in the chamber. The relationship between composition and hygroscopicity of SOA and how organic aerosols with high hygroscopicity are generated in the real atmosphere need to be further studied.

## Supporting materials

Supplementary data associated with this article can be found in the online version.

REFERENCES

Baltensperger U, Kalberer M, Dommen J, Paulsen D, Alfarra M R, Coe H et al., 2005. Secondary organic aerosols from anthropogenic and biogenic precursors. *Faraday Discussions*, 130: 265–278.

Broday D M, Georgopoulos P G, 2001. Growth and deposition of hygroscopic particulate matter in the human lungs. *Aerosol Science and Technology*, 34: 144–159.

Cappa C D, Che D L, Kessler S H, Kroll J H, Wilson K R, 2011. Variations in organic aerosol optical and hygroscopic properties upon heterogeneous OH oxidation. *Journal of Geophysical Research-Atmospheres*, 116.

Chu B, Hao J, Takekawa H, Li J, Wang K, Jiang J, 2012. The remarkable effect of FeSO$_4$ seed aerosols on secondary organic aerosol formation from photooxidation of α-pinene/NO$x$ and toluene/NO$x$. *Atmospheric Environment*, 55: 26–34.

Chu B, Hao J, Li J, Takekawa H, Wang, Jiang J, 2013. Effects of two transition metal sulfate salts on secondary organic aerosol formation in toluene/NO($x$) photooxidation. *Frontiers of Environmental Science & Engineering*, 7: 1–9.

Cocker D R, Mader B T, Kalberer M, Flagan R C, Seinfeld J H, 2001. The effect of water on gas-particle partitioning of secondary organic aerosol: II. *m*-xylene and 1,3,5-trimethylbenzene photooxidation systems. *Atmospheric Environment*, 35: 6073–6085.

Cruz C N, Pandis S N, 2000. Deliquescence and hygroscopic growth of mixed inorganic-organic atmospheric aerosol. *Environmental Science & Technology*, 34: 4313–4319.

Dick W D, Saxena P, McMurry P H, 2000. Estimation of water uptake by organic compounds in submicron aerosols measured during the Southeastern Aerosol and Visibility Study. *Journal of Geophysical Research D: Atmospheres*, 105: 1471–1479.

Duplissy J, Gysel M, Alfarra M R, Dommen J, Metzger A, Prevot A S H et al., 2008. Cloud forming potential of secondary organic aerosol under near atmospheric conditions. *Geophysical Research Letters*, 35(1): L03818.

Flores J M, Bar-Or R Z, Bluvshtein N, Abo-Riziq A, Kostinski A, Borrmann S et al., 2012. Absorbing aerosols at high relative humidity: linking hygroscopic growth to optical properties. *Atmospheric Chemistry and Physics*, 12: 5511–5521.

Gao S, Ng N L, Keywood M, Varutbangkul V, Bahreini R, Nenes A, et al., 2004. Particle phase acidity and oligomer formation in secondary organic aerosol. *Environmental Science & Technology*, 38: 6582–6589.

Gysel M, Weingartner E, Nyeki S, Paulsen D, Baltensperger U, Galambos I et al., 2004. Hygroscopic properties of water-soluble matter and humic-like organics in atmospheric fine aerosol. *Atmospheric Chemistry and Physics*, 4: 35–50.

Hamilton J F, Webb P J, Lewis A C, Reviejo M M, 2005. Quantifying small molecules in secondary organic aerosol formed during the photo-oxidation of toluene with hydroxyl radicals. *Atmospheric Environment*, 39: 7263–7275.

Heintzenberg J, Maβling A, Birmili W, 2001. The connection between hygroscopic and optical particle properties in the atmospheric aerosol. *Geophysical Research Letters*, 28: 3649–3651.

IPCC, 2013. Working group I contribution to the IPCC fifth Assessment Report (AR5), climate change 2013: the physical science basis, Geneva, Switzerland.

Jang M S, Czoschke N M, Lee S, Kamens R M, 2002. Heterogeneous atmospheric aerosol production by acid-catalyzed particle-phase reactions. *Science*, 298: 814–817.

Juranyi Z, Gysel M, Duplissy J, Weingartner E, Tritscher T, Dommen J et al., 2009. Influence of gas-to-particle partitioning on the hygroscopic and droplet activation behaviour of alpha-pinene secondary organic aerosol. *Physical Chemistry Chemical Physics*, 11: 8091–8097.

Kroll J H, Chan A W H, Ng N L, Flagan R C, Seinfeld J H, 2007. Reactions of semivolatile organics and their effects on secondary organic aerosol formation. *Environmental Science & Technology*, 41: 3545–3550.

Lu Z F, Hao J M, Takekawa H, Hu L H, Li J H, 2009. Effect of high concentrations of inorganic seed aerosols on secondary organic aerosol formation in the *m*-xylene/NO$x$ photooxidation system. *Atmospheric Environment*, 43: 897–904.

Ma Q X, Liu Y C, He H, 2010. The utilization of physisorption analyzer for studying the hygroscopic properties of atmospheric relevant particles. *Journal of Physical Chemistry A*, 114: 4232–4237.

Meyer N K, Duplissy J, Gysel M, Metzger A, Dommen J, Weingartner E et al., 2009. Analysis of the hygroscopic and volatile properties of ammonium sulphate seeded and unseeded SOA particles. *Atmospheric Chemistry and Physics*, 9: 721–732.

Michaud V, El Haddad I, Liu Y, Sellegri K, Laj P, Villani P et al., 2009. In-cloud processes of methacrolein under simulated conditions–Part 3: Hygroscopic and volatility properties of the formed secondary organic aerosol. *Atmospheric Chemistry and Physics*, 9: 5119–5130.

Mochida M, Miyakawa T, Takegawa N, Morino Y, Kawamura K, Kondo Y, 2008. Significant alteration in the hygroscopic properties of urban aerosol particles by the secondary formation of organics. *Geophysical Research Letters*, 35(2): L02804.

Ng N L, Herndon S C, Trimborn A, Canagaratna M R, Croteau P L, Onasch T B et al., 2011. An Aerosol Chemical Speciation Monitor (ACSM) for routine monitoring of the composition and mass concentrations of ambient aerosol. *Aerosol Science and Technology*, 45: 770–784.

Odum J R, Hoffmann T, Bowman F, Collins D, Flagan R C, Seinfeld J H, 1996. Gas/particle partitioning and secondary organic aerosol yields. *Environmental Science & Technology*, 30: 2580–2585.

Petters M D, Kreidenweis S M, 2007. A single parameter representation of hygroscopic growth and cloud condensation nucleus activity. *Atmospheric Chemistry and Physics*, 7: 1961–1971.

Prisle N L, Engelhart G J, Bilde M, Donahue N M, 2010. Humidity influence on gas-particle phase partitioning of alpha-pinene + O$_3$ secondary organic aerosol. *Geophysical Research Letters*, 37: L01802.

Quinn P K, Bates T S, Baynard T, Clarke A D, Onasch T B, Wang W et al., 2005. Impact of particulate organic matter on the relative humidity dependence of light scattering: A simplified parameterization. *Geophysical Research Letters*, 32: 1–4.

Stokes R H, Robinson R A, 1966. Interactions in aqueous nonelectrolyte solutions. I. Solute-solvent equilibria. *Journal of Physical Chemistry*, 70: 2126–2131.

Takekawa H, Karasawa M, Inoue M, Ogawa T, Esaki Y, 2000. Product analysis of the aerosol produced by photochemical reaction of α-pinene. *Earozoru Kenkyu*, 15: 35–42.

Takekawa H, Minoura H, Yamazaki S, 2003. Temperature dependence of secondary organic aerosol formation by photo-oxidation of hydrocarbons. *Atmospheric Environment*, 37: 3413–3424.

Tritscher T, Dommen J, DeCarlo P F, Gysel M, Barmet P B, Praplan A P et al., 2011. Volatility and hygroscopicity of aging secondary organic aerosol in a smog chamber. *Atmospheric Chemistry and Physics* , 11: 11477–11496.

Ulbrich I M, Canagaratna M R, Zhang Q, Worsnop D R, Jimenez J L, 2009. Interpretation of organic components from positive matrix factorization of aerosol mass spectrometric data. *Atmospheric Chemistry and Physics*, 9: 2891–2918.

Varutbangkul V, Brechtel F J, Bahreini R, Ng N L, Keywood M D,

Kroll J H et al., 2006. Hygroscopicity of secondary organic aerosols formed by oxidation of cycloalkenes, monoterpenes, sesquiterpenes, and related compounds. *Atmospheric Chemistry and Physics*, 6: 2367–2388.

Virkkula A, Van Dingenen R, Raes F, Hjorth J, 1999. Hygroscopic properties of aerosol formed by oxidation of limonene, alpha-pinene, and beta-pinene. *Journal of Geophysical Research-Atmospheres*, 104: 3569–3579.

Wu S, Lu Z F, Hao J M, Zhao Z, Li J H, Hideto T, Hiroaki M, Akio Y, 2007. Construction and characterization of an atmospheric simulation smog chamber. *Advances in Atmospheric Sciences*, 24: 250–258.

Xiong J Q, Zhong M, Fang C, Chen LC, Lippmvann M, 1998. Influence of organic films on the hygroscopicity of ultrafine sulfuric acid aerosol. *Environmental Science and Technology*, 32: 3536–3541.